

Wave behavior at the interface of inviscid fluid and NL bio-thermoelastic diffusive media

Rajneesh Kumar^{1a}, Suniti Ghangas^{*2} and Anil K. Vashishth^{1b}

¹Department of Mathematics, Kurukshetra University, Kurukshetra, 136119 Haryana, India

²Department of Mathematics, M.D.S.D. Girls College, Ambala City, 134003, Haryana, India

(Received August 26, 2020, Revised January 5, 2021, Accepted January 20, 2021)

Abstract. This work throws light on the reflection and transmission phenomenon due to incident plane longitudinal wave at a plane interface between inviscid fluid half-space and a nonlocal bio-thermoelastic diffusive half-space. The governing equations are formulated by adopting nonlocal heat conduction and mass diffusion along with dual phase lag (DPL) model. The amplitude ratios are obtained analytically and these amplitude ratios are used to drive energy ratios. The distribution of energy of incident wave among reflected and transmitted waves are obtained. The obtained ratios are impacted by angle of incidence, frequency and different properties of media involved. Numerically examined energy ratios are displayed in the form of graphs to know the effect of nonlocal parameters, lagging times, stiffness and blood perfusion rate.

Keywords: amplitude ratios; bio-thermoelasticity; diffusion; fluid; non local; reflection; transmission

1. Introduction

In clinical treatment, a lot of modern thermo-therapeutics (microwave, laser, focused ultrasound, and radio-frequency) have been widely used. For example, the laser is focused on tumor by an objective lens for thermal therapy. During thermal therapy, delivering the appropriate heat energy to the infected tissue without affecting the healthy tissue is the biggest challenge. Thus an acute need is to understand how the temperature/stress fields affect the kinetics of a thermal treatment.

In living biological tissues, heat transfer analysis is a complicated physiological process due to the inherent characteristics in tissues, e.g. blood circulation, sweating, metabolic heat generation, and heat dissipation via hair or fur. Pennes (1958) established the bioheat transfer model to describe this complex phenomena which is based on Fourier's law of heat conduction. So far lots of research work is done based on Cattaneo (1958), Vernotte (1958) and Tzou (1995) models of heat conduction to understand the thermal behavior of biological tissues.

Later, Roychoudhuri (2007) extended the idea of Tzou on Green Nagdhi III by introducing the third phase-lag τ_v in correspondence to thermal displacement and developed another generalized

*Corresponding author, E-mail: sunitikuk@gmail.com

^aProfessor, E-mail: rajneesh_kuk@rediffmail.com

^bProfessor, E-mail: akvashishth@kuk.ac.in

thermoelastic theory, three phase lag (TPL) thermo-elastic theory. Kumar *et al.* (2019a) and (Kumar and Rai 2020) used this TPL theory to investigate the behavior of skin tissue. The theory of coupled thermoelasticity was expanded by Lord and Shulman (1967) and Green and Lindsay (1972). Chen *et al.* (1968) and Chen *et al.* (1969) developed a new theory of thermoelasticity with two temperature. A comprehensive work have been done by using these theories by various investigators (Lotfy (2014), Lotfy and Hassan (2014), Othman *et al.* (2011), Othman *et al.* (2014)).

Thermomass is defined according to Einstein's mass-energy relation as the equivalent mass of phonon gas in dielectrics. The concept of thermal as well as mechanical fields are employed in the thermomass heat conduction theory. This theory is used to study the heat at micro to nano scale and Cao *et al.* (2007), Guo *et al.* (2008) and Guo *et al.* (2010) used this theory. Tzou and Guo (2010) developed new heat conduction law which consider nonlocal behavior with thermal lagging. Wang *et al.* (2014) proposed , a new theory of generalized thermoelasticity by taking into account the general heat conduction law depending thermomass theory. Sarkar (2019) formulated the new governing equations of thermoelasticity with nonlocal heat conduction. Yu *et al.* (2016) investigated that the model of Guyer and Krumhansl (1966) is the potential model for heat conduction at nano scale and Kumar *et al.* (2019b) extended the GK model to nonlocal dual-phase-lag (NL DPL) model in a bi-layer tissue during magnetic fluid hyperthermia.

Some authors worked on the thermo-mechanical behavior of tissues. Xu *et al.* (2008) investigated the heat transfer, thermal damage and heat-induced stress of human skin. Kim *et al.* (2016) analyzed the transient thermal-mechanical responses of innocuous tactile stimulation induced by laser. Shen *et al.* (2005) developed a tissue damage model using Fourier bio-heat transfer equation. It shows that thermally induced mechanical deformation decreases the activation energy for protein denaturation, making soft tissues more easily to be damaged. Li *et al.* (2014) and Li *et al.* (2016) developed a model to predict thermally induced mechanical deformation and thermal damage of soft tissues by combining the Fourier and non Fourier bio-heat transfer equation with the theory of linear thermo-elasticity.

Park *et al.* (2017) presented a thermoelastic deformation model of tissue contraction during thermal ablation. Li *et al.* (2018) used the generalized thermoelastic theory without energy dissipation to investigate bioheat transfer and heat-induced mechanical response in bi-layered human skin with variable thermal material properties.

Li *et al.* (2018) developed the theory of modified fractional order generalized bio-thermoelasticity with material properties. Ghanmi and Abbas (2019) studied the thermal damage during the thermal therapy within the skin tissue by using bioheat equation.

In order to analyse the behavior of waves at the interface of half space, Sharma *et al.* (2014) investigated the problem of reflection and transmission of plane waves at an imperfect boundary between two thermally conducting micropolar elastic solid half spaces with two temperature. Sharma (2012) examined the reflection of plane waves from a free surface of a thermodiffusive elastic half space with void.

The present work is devoted to investigate the phenomenon of reflection and transmission of plane waves from the interface between fluid half space and nonlocal bio-thermoelastic diffusive half space. The effect of nonlocal parameters, lagging time, blood perfusion rate and stiffness parameter on energy ratios is discussed and presented graphically. The conservation of energy at the interface is verified.

2. Modeling equations

Following Sherief (2004) and Xiong and Guo (2017), the basic equations for a homogeneous, isotropic, nonlocal bio-thermoelastic diffusive medium in the absence of body forces, external heat sources and mass diffusion source are as follows.

2.1 Constitutive equations

$$\sigma_{ij} = 2\mu e_{ij} + \delta_{ij}(\lambda_0 e_{kk} - \gamma_1 \theta - \gamma_2 P), \quad (1)$$

$$C = \gamma_2 e_{kk} + d\theta + nP, \quad (2)$$

$$\rho S = \gamma_1 e_{kk} + l_1 \theta + dP, \quad (3)$$

where $\theta = T - T_0$ denote the increment of temperature, T is the absolute temperature, T_0 is the initial reference temperature, λ , μ are Lamé's constants. e_{ij} , P , C and S are separately the components of strain tensor, chemical potential, concentration of diffusive materials and the entropy density.

Following Yu *et al.* (2016), Xiong and Guo (2017) and Kumar *et al.* (2019b) and using the above set of equations, we have the following nonlocal equations.

Nonlocal equations of motion

$$(1 - \xi^2 \nabla^2)(\rho \ddot{\mathbf{u}}) = \mu \nabla^2 \mathbf{u} + (\lambda_0 + \mu) \nabla \nabla \cdot \mathbf{u} - \gamma_1 \nabla \theta - \gamma_2 \nabla P. \quad (4)$$

Nonlocal bioheat transfer equation

$$(1 - \zeta^2 \nabla^2 + \tau_q \frac{\partial}{\partial t} + \frac{\tau_q^2}{2} \frac{\partial^2}{\partial t^2})[\gamma_1 T_0 \dot{e}_{kk} + l_1 T_0 \dot{\theta} + d T_0 \dot{P} - \omega_b \rho_b c_b \theta] = k(1 + \tau_T \frac{\partial}{\partial t}) \nabla^2 \theta. \quad (5)$$

Nonlocal mass diffusion equation

$$(1 - \zeta^2 \nabla^2 + \tau_v \frac{\partial}{\partial t} + \frac{\tau_v^2}{2} \frac{\partial^2}{\partial t^2})[\gamma_2 \dot{e}_{kk} + d \dot{\theta} + n \dot{P}] = D(1 + \tau_P \frac{\partial}{\partial t}) \nabla^2 P, \quad (6)$$

where ∇^2 is Laplacian operator.

Following Achenbach (1973), the constitutive relations for the inviscid fluid half space are

$$\sigma_{ij}^f = \lambda^f u_{k,k}^f \delta_{ij}, \quad (i, j, k = 1, 2, 3), \quad (7)$$

and equations of motion are

$$\sigma_{ij,j}^f - \rho^f \ddot{u}_i^f = 0. \quad (i, j = 1, 2, 3), \quad (8)$$

where

$$\lambda_0 = \lambda - \frac{\beta_2^2}{b}, \gamma_1 = \beta_1 + \frac{a}{b} \beta_2, \gamma_2 = \frac{\beta_2}{b},$$

$$l_1 = \frac{\rho C}{T_0} + \frac{a^2}{b}, = \frac{a}{b}, = \frac{1}{b},$$

$$\beta_1 = (3\lambda + 2\mu)\alpha_t, \beta_2 = (3\lambda + 2\mu)\alpha_c.$$

3. Statement of the problem

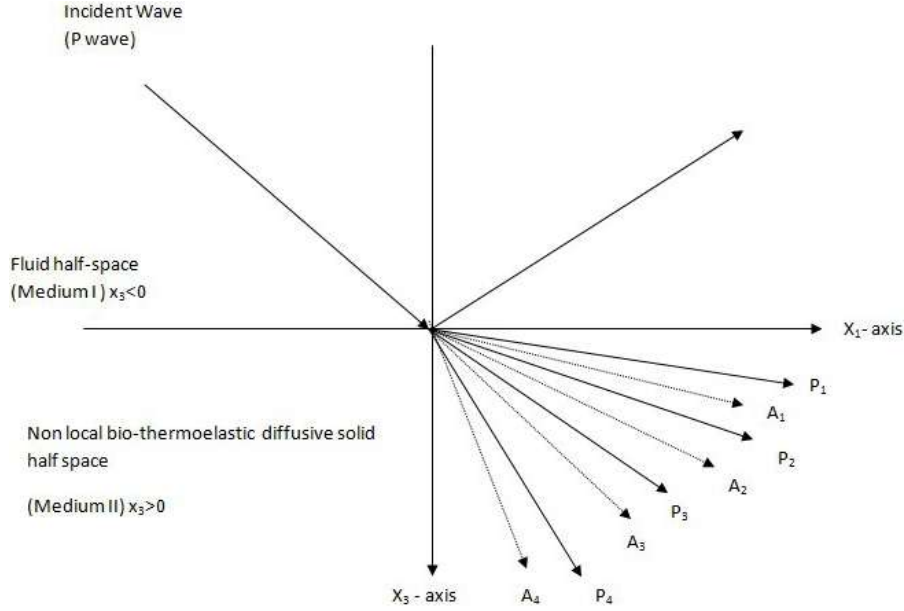


Fig. 1 Geometry of the problem

We consider an inviscid fluid half-space (FS) and a nonlocal isotropic bio-thermoelastic diffusive half space (NL BDS) as shown in the Fig. 1. The FS occupies the region $x_3 \leq 0$ and NL BDS occupies the region $x_3 \geq 0$.

Introducing the following dimensionless quantities

$$(x_i, u_i, \xi', \zeta', \vartheta') = \frac{\omega_1^*}{c_0} (x_i, u_i, \xi, \zeta, \vartheta),$$

$$(t', \tau_q, \tau_p, \tau_v, \tau_T) = \omega_1^* (t, \tau_q, \tau_p, \tau_v, \tau_T),$$

$$u_i^{f'} = \frac{u_i^f}{c_0}, \quad \theta' = \frac{\gamma_1}{\rho c_0^2} \theta, \quad P' = \frac{P}{b\gamma_2},$$

$$P^{*f'} = \frac{P^{*f}}{\gamma_1 T_0 c_1}, \quad \sigma_{33}^{f'} = \frac{\sigma_{33}^f}{\gamma_1 T_0}, \quad k_{n'} = \frac{c_0}{\gamma_1 T_0} k_n,$$

where $c_0^2 = \frac{\lambda+2\mu}{\rho}$, $\omega_1^* = \frac{\rho c c_0^2}{k}$, $i = 1, 3$.

The Helmholtz representation of the dimensionless components of the displacement vector $\mathbf{u} = (u_1, 0, u_3)$ in NL BDS and velocity vector $\mathbf{u}^f = (u_1^f, 0, u_3^f)$ in FS and for two dimensional problem can be expressed in terms of the potential functions as follows

$$u_1 = \frac{\partial \phi}{\partial x_1} - \frac{\partial \psi}{\partial x_3}, \quad u_3 = \frac{\partial \phi}{\partial x_3} + \frac{\partial \psi}{\partial x_1}, \quad (9)$$

$$u_1^f = \frac{\partial \phi^f}{\partial x_1}, \quad u_3^f = \frac{\partial \phi^f}{\partial x_3}. \quad (10)$$

The following relation is used for the propagation of harmonic wave in $x_1 - x_3$ plane

$$(\phi, \psi, \theta, P, \psi^f)(x_1, x_3, t) = (\bar{\phi}, \bar{\psi}, \bar{\theta}, \bar{P}, \bar{\psi}^f)e^{-i\omega t}, \quad (11)$$

where ω is the angular frequency and the potential $\bar{\phi} = \bar{\phi}_1 + \bar{\phi}_2 + \bar{\phi}_3$ is determined from the following wave equation

$$(\nabla^2 + \frac{\omega^2}{V_i^2})\bar{\phi}_i = 0, i = 1,2,3, \quad (12)$$

where $V_i, i = 1,2,3$ are the velocities of the three longitudinal waves, that is, P, T (Thermal) and MD (Mass Diffusive) waves, which are derived from the roots of the following cubic equation

$$B_4V^6 - B_3\omega^2V^4 + B_2\omega^4V^2 - B_1\omega^6 = 0, \quad (13)$$

where the coefficients $B_i, i=1,2,3,4$ are given in the Appendix B.

The potentials $\bar{\psi}$ is determined from the wave Eq. (14)

$$(\nabla^2 + \frac{\omega^2}{V_4^2})\bar{\psi} = 0, \quad (14)$$

where $V_4 = \delta$ is the velocity of the transverse wave.

Following Borchardt (1982), potential functions in NL BDS are defined as

$$(\phi, \theta, P) = \sum_{i=1}^3 (1, n_i, k_i)D_i \exp(\mathbf{A}_i \cdot \mathbf{r}) \exp(i(\mathbf{P}_i \cdot \mathbf{r} - \omega t)), \quad (15)$$

$$\psi = D_4 \exp(\mathbf{A}_4 \cdot \mathbf{r}) \exp(i(\mathbf{P}_4 \cdot \mathbf{r} - \omega t)). \quad (16)$$

The coefficients $D_i, i=1, 2, 3, 4$ represent the amplitudes of refracted P, MD, T and SV-waves, respectively. The propagation vector $\mathbf{P}_i, i = 1, 2, 3, 4$ and attenuation factor $\mathbf{A}_i, i = 1, 2, 3, 4$ are given by

$$\mathbf{P}_i = \xi_{ir}\hat{x}_1 + dV_{ir}\hat{x}_3, \mathbf{A}_i = -\xi_{im}\hat{x}_1 - dV_{im}\hat{x}_3, i = 1,2,3,4, \quad (17)$$

where

$$dV_i = dV_{ir} + idV_{im} = p.v. (\frac{\omega^2}{V_i} - \xi^2)^{\frac{1}{2}}, i = 1,2,3,4. \quad (18)$$

$\xi = \xi_{ir} + i\xi_{im}$ is a complex wave number. The subscripts ir and im denote the real and imaginary parts of the corresponding complex quantity respectively and p.v. denotes the principal value of the complex quantity, $\xi_{ir} \geq 0$ denotes the propagation in the positive direction x_1 , and the complex number ξ is determined as

$$\xi = |\mathbf{P}_i|\sin(\theta_i^*) - i|\mathbf{A}_i|\sin(\theta_i^* - \gamma_i), \quad (19)$$

where $\gamma_i (i = 1,2,3,4)$ is the angle between the propagation and attenuation waves and $\theta_i^* (i=1,2,3,4)$ is the angle of refraction of the incident wave in NL BDS.

4. Reflection and transmission

We consider a plane harmonic wave (P) propagating through the inviscid fluid half-space and is incident at the interface $x_3 = 0$. Corresponding to the incident wave, one homogeneous wave (P) is reflected in FS and four inhomogeneous waves (P, T, MD and SV) are transmitted in NL BDS. In inviscid fluid half-space, the potential function can be written as

$$\phi^f = B_0^f \exp[i\omega(\frac{x_1 \sin(\theta_0) + x_3 \cos(\theta_0)}{c_p^f} - t)] + B_1^f \exp[i\omega(\frac{x_1 \sin(\theta_1) + x_3 \cos(\theta_1)}{c_p^f} - t)]. \quad (20)$$

The coefficients B_0^f and B_1^f are amplitudes of the incident P and reflected P waves, respectively.

4.1 Boundary conditions

We consider two bounded half-spaces. If the boundary is imperfect and the size and spacing between the imperfection is much smaller than the wave length then at the interface $x_3 = 0$, following Lavrentyev and Rokhlin (1998) these can be described by using boundary conditions.

(i) The condition of continuity of the stress components

$$\sigma_{33} = -p^f, \quad \sigma_{31} = 0; \quad (21)$$

(ii) Discontinuity of the normal stress across the interface is

$$\sigma_{33} = k_n(u_{3(M_1)}^f - \dot{u}_{3(M_2)}); \quad (22)$$

(iii) Condition of thermal insulation of the boundary

$$\frac{\partial \theta}{\partial x_3} = 0; \quad (23)$$

(iv) Condition of impermeability of the boundary

$$\frac{\partial P}{\partial x_3} = 0. \quad (24)$$

We obtain the following system of five non-homogeneous equations in five unknowns by using the boundary conditions

$$\sum_{j=1}^5 d_{ij} Z_j = g_i, \quad (25)$$

with the Snell's law

$$\xi_{ir} = \frac{\omega \sin(\theta_0)}{c_p^f} = \frac{\omega \sin(\theta_1)}{c_p^f}, \quad (26)$$

where Z_j ($j=1,2,3,4,5$) are the ratios between the amplitudes of the reflected waves P and SV , refracted waves P, T, MD and SV waves and the amplitude of the incident wave, the values of d_{ij} ($i, j=1,2,3,4,5$) are given in Appendix C and $\xi_{im} = 0$. The coefficients g_i ($i=1,2,3,4,5$) in the R.H.S. of Eq. (25) are determined as

$$g_i = \begin{cases} d_{11}, & \text{for } i = 1, \\ 0, & \text{for } i = 2, 3, 4, 5. \end{cases} \quad (27)$$

Following Achenbach (1973), the field equations can be expressed in terms of velocity potential for inviscid fluid as

$$p^f = -\rho^f \dot{\phi}^f. \quad (28)$$

$$\left(\nabla^2 - \frac{1}{(\alpha_p^f)^2} \frac{\partial^2}{\partial t^2}\right)\phi^f = 0. \quad (29)$$

$$\mathbf{u}^f = \nabla\phi^f. \quad (30)$$

Applying the dimensionless quantities, we have

$$p^f = -\xi_1 \dot{\phi}^f, \quad (31)$$

$$\left(\nabla^2 - \frac{1}{(c_p^f)^2} \frac{\partial^2}{\partial t^2}\right)\phi^f = 0, \quad (32)$$

where

$$\xi_1 = \frac{\rho^f c_1^2}{\beta_1 T_0}, \quad c_p^f = \frac{\alpha_p^f}{c_1}, \quad (\alpha_p^f)^2 = \frac{\lambda^f}{\rho^f},$$

and λ^f is the bulk modulus, ρ^f is the density of the liquid, u^f is the velocity vector and p^f is the acoustic pressure of the inviscid fluid.

To calculate the partition of energy of the incident wave among the reflected and transmitted waves on both sides of the surface, we consider a surface element of unit area. Following Achenbach (1973), the representation of the energy flux across the surface element is

$$P^* = \sigma_{ij} l_j \dot{u}_i, \quad (33)$$

where σ_{ij} is stress tensor, l_j are direction cosine of unit normal \hat{l} outward of surface element and \dot{u}_j are the components of the particle velocity.

The average energy intensities of the waves in the FS on the surface with normal along x_3 -direction are given by

$$\langle P^{*f} \rangle = \text{Re} \langle p^f \rangle \cdot \text{Re} \langle u_3^f \rangle, \quad (34)$$

where, $\langle P^* \rangle$ denotes the time average of P^* , represents the average energy transmission per unit surface area per unit time and for any two complex functions f and g , we have

$$\langle \text{Re}(f), \text{Re}(g) \rangle = \text{Re}(f, \bar{g})/2. \quad (35)$$

The expression for energy ratio E_1 for the reflected P wave is given by

$$E_1 = -\frac{\langle P^{*f} \rangle}{\langle P_0^{*f} \rangle}, \quad (36)$$

where

$$\langle P^{*f} \rangle = -(\xi_1 \omega^2 / (2c_p^f)) |Z_1|^2 \text{Re}(\cos(\theta_1)), \quad (37)$$

and for incident P-wave is

$$\langle P_0^{*f} \rangle = -\left(\frac{\xi_1 \omega^2}{2c_p^f}\right) \cos(\theta_0), \quad (38)$$

are the average energy intensities of the reflected P- and incident P- , respectively. In Eq. (37), negative sign is taken because the direction of reflected waves is opposite to that of incident wave. For NL BDS, the average intensities of the waves on the surface with normal along x_3 -direction, are given by

$$\langle P_{ij}^* \rangle = \text{Re}(\langle \sigma_{13}^i \rangle) \text{Re}(\langle \dot{u}_1^j \rangle) + \text{Re}(\langle \sigma_{33}^i \rangle) \text{Re}(\langle \dot{u}_3^j \rangle). \quad (39)$$

The expressions for energy ratios for the refracted P-, refracted MD-, refracted T- and refracted SV- waves are given by

$$E_{ij} = \frac{\langle P_{ij}^* \rangle}{\langle P_0^{*f} \rangle}, i, j = 1, 2, 3, 4. \quad (40)$$

The diagonal entries of energy matrix E_{ij} in Eq. (40) represents the energy ratios of P, T, MD-SV- waves respectively, whereas sum of the non diagonal entries of E_{ij} give the share of interaction energy among all refracted waves in the medium and is given by

$$E_{RR} = \sum_{i=1}^3 \left(\sum_{j=1}^3 E_{ij} - E_{ii} \right). \quad (41)$$

The energy ratio E_1 , diagonal entries of the matrix E_{ij} and E_{RR} yield the conservation of incident energy across the interface, through the relation

$$E_1 + E_2 + \sum_{i=1}^4 E_{ii} + E_{RR} = 1. \quad (42)$$

4.2 Validation

In the absence of metabolic heat source ($\omega_b = 0$), nonlocal parameters ($\xi = 0, \zeta = 0, \varsigma = 0$), the problem reduced to the reflection and transmission of P wave at the interface of inviscid fluid and thermoelastic diffusive media with the changed value of $d_{31} = i \frac{dV_\alpha}{\omega}$, $d_{3j} = -\frac{dV_j}{\omega}$, $d_{35} = -\frac{\xi_R}{\omega}$ where $j=2,3,4$. The results obtained are in agreement with the results of Kumar and Gupta (2015) which leads to the validation of our results.

5. Results and discussion

In this work, the energy ratios for ES and BDS are obtained for the different angle of incidence. The computation has been made using MATLAB (R2016a) software and the results are presented graphically. The numerical data for parameters of blood, parameters of diffusion, material constants, nonlocal parameters are given in Tables 1-4 respectively. The values of other parameters are given in figures.

Table 1 Parameters of blood (Kumar *et al.* 2019b)

Parameters	Units	Values
ρ_b	kgm^{-3}	1060
c_b	$\text{Jkg}^{-1}\text{K}^{-1}$	3600
ω_b	$\text{Wm}^{-1}\text{K}^{-1}$	1.87×10^{-3}

Table 2 Diffusion parameters (Xiong and Guo 2017)

Parameters	Units	Values
D	kgsm^{-3}	0.85×10^{-8}
a	$\text{m}^2\text{s}^{-2}\text{K}^{-1}$	1.2×10^4
b	$\text{kg}^{-1}\text{s}^{-2}\text{m}^5$	9×10^5

Table 3 Material Constants (Li *et al.* 2018)

Parameters	Units	Values
λ	$\text{kgm}^{-1}\text{s}^{-2}$	8.27×10^8
μ	$\text{kgm}^{-1}\text{s}^{-2}$	3.446×10^7
α	K^{-1}	1×10^{-4}
ρ	kgm^{-3}	1190
c	$\text{Jkg}^{-1}\text{K}^{-1}$	4196

Table 4 Nonlocal parameters (Kumar *et al.* 2019b)

Parameters	Units	Values
ξ	m	0.02
ζ	m	0.02
ϑ	m	0.02

Fig. 2 shows the effects of blood perfusion rate ω_b on energy ratios along angle of incidence. Fig. 2(a) shows that energy ratio E_{11} decreases for $\omega_b = 1.87 \times 10^{-3}$ to $\omega_b = 3.87 \times 10^{-3}$ but for $\omega_b = 4.87 \times 10^{-3}$ the profile of E_{11} increases. Other energy ratios show similar behavior as shown in Fig. 2(b)-2(d). From these figures it is noticed that for $\omega_b = 1.87 \times 10^{-3}$ energy ratios are almost zero but as ω_b the profile of energy ratios show the constant behavior.

Fig. 3 shows the effect of stiffness parameter k_n on the energy ratios along angle of incidence. Fig. 3(a) shows that the energy ratio E_1 increases along the angle of incidence θ_0 and the E_1 profile decreases as the value of stiffness parameter k_n increases. From the Fig. 3(b) it is noticed that as the value of k_n increases profile of E_{11} also increases and each profile increases for $0^\circ \leq \theta_0 \leq 45^\circ$ and decreases for $45^\circ \leq \theta_0 \leq 90^\circ$. Energy ratios E_{22} , E_{33} and E_{44} show the same behavior as of E_{11} . The behavior of E_{22} increases for $0^\circ \leq \theta_0 \leq 45^\circ$ and decreases for $45^\circ \leq \theta_0 \leq 90^\circ$. E_{33} increases for $0^\circ \leq \theta_0 \leq 55^\circ$ and decreases for $55^\circ \leq \theta_0 \leq 90^\circ$. E_{44} increases for $0^\circ \leq \theta_0 \leq 65^\circ$ and decreases for $65^\circ \leq \theta_0 \leq 90^\circ$.

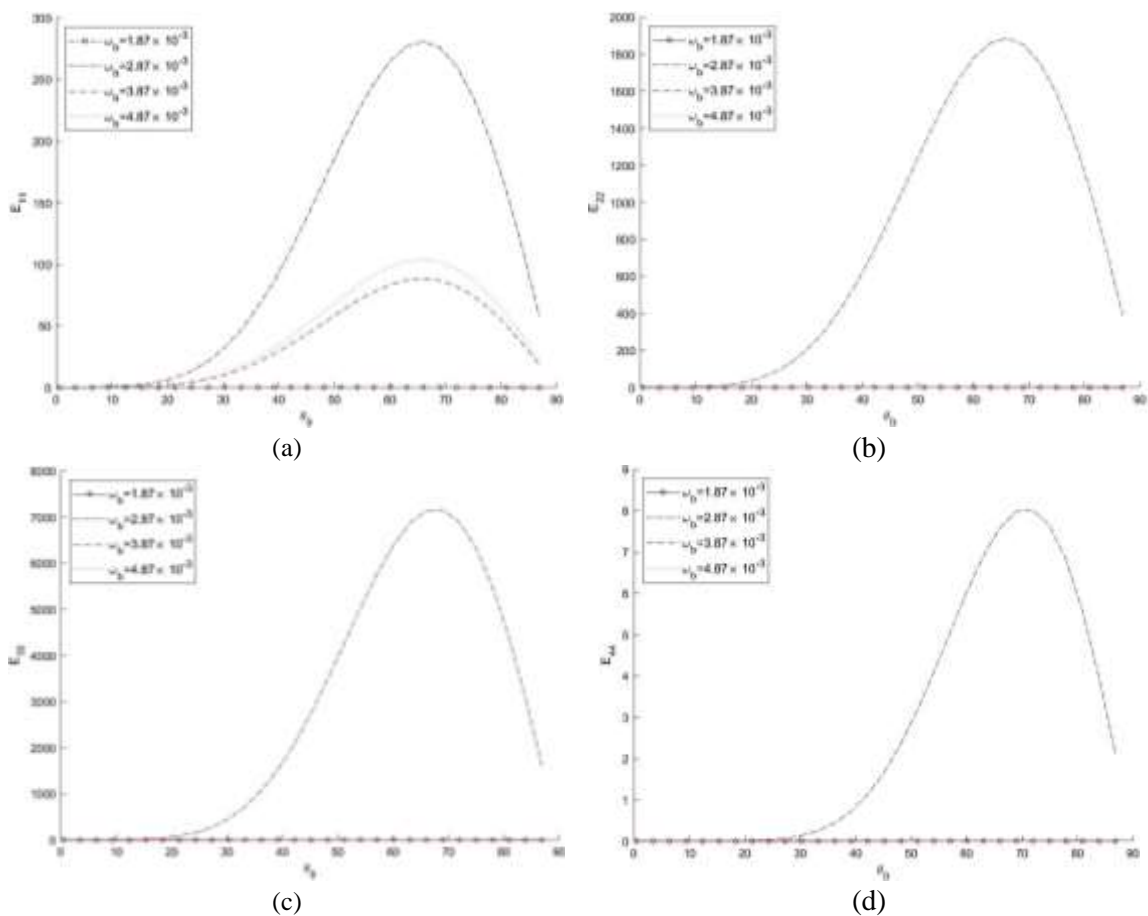


Fig. 2 Effect of blood perfusion rate ω_b on energy ratios

Fig. 4 shows the effect of nonlocal parameters ξ , ζ , and ς on the energy ratios along angle of incidence. From these figures it is observed that as the value of nonlocal parameters increases the energy ratios profile E_{11} , E_{22} , E_{33} , and, E_{44} decreases. The trend of energy ratios (E_{11}, E_{22}) is similar and (E_{33}, E_{44}) is similar.

Fig. 5 shows the effect of phase lag parameters on the energy ratios along angle of incidence. It is clear from the figure that behavior of all energy ratios is same but with different magnitude values. The energy ratios achieved maximum value near the 65° of angle of incidence.

6. Conclusions

In this work, the reflection and transmission phenomena of plane waves from the interface between the FS and NL BDS is studied. In NL BDS the four basic waves are found to vibrate with distinct speed. The speed of propagation of all the waves are found to be complex valued and frequency dependent. Numerical results show that the energy ratios of various reflected and transmitted waves are affected significantly by non local, phase lag, stiffness parameters and blood

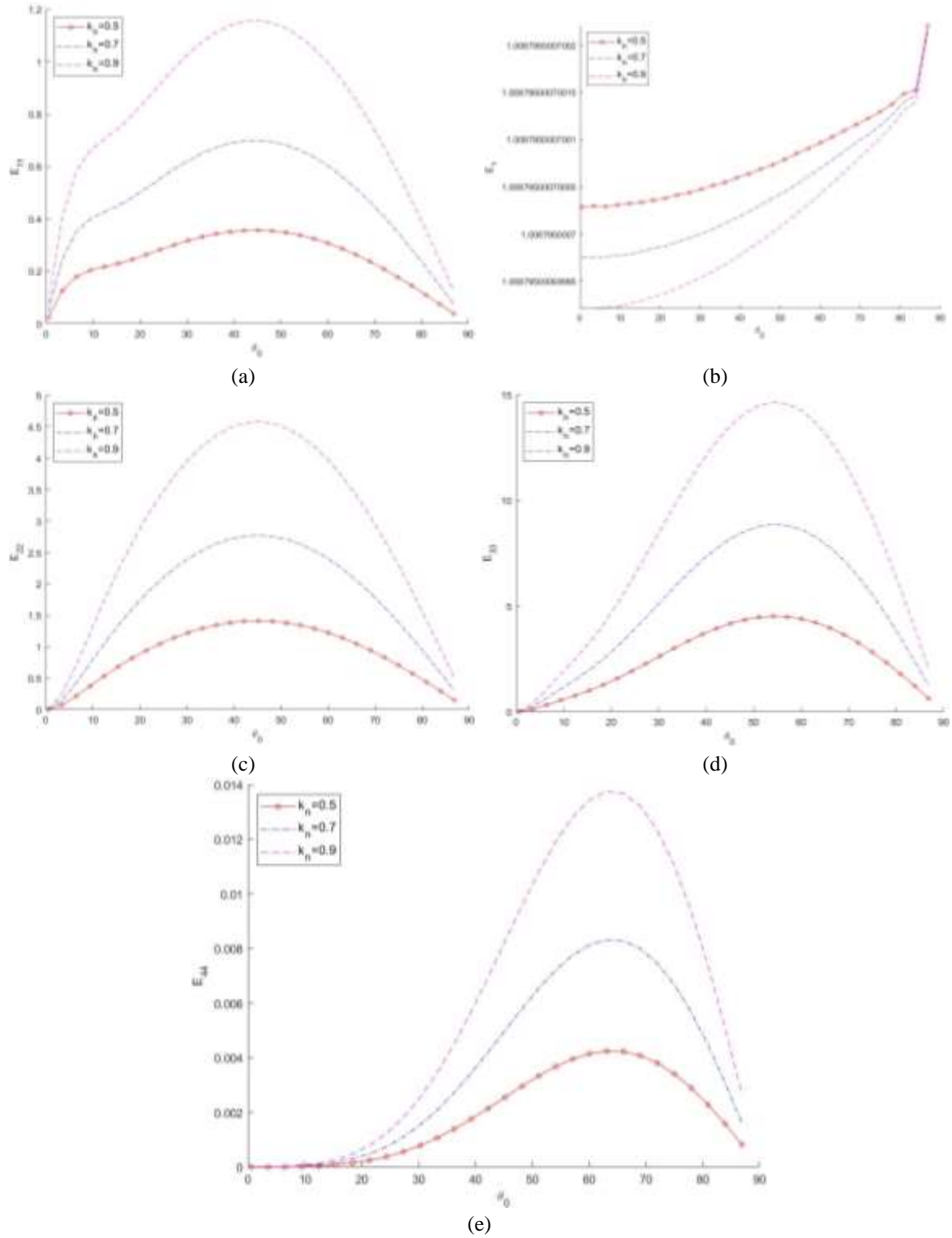


Fig. 3 Effect of stiffness parameter k_n on energy ratios

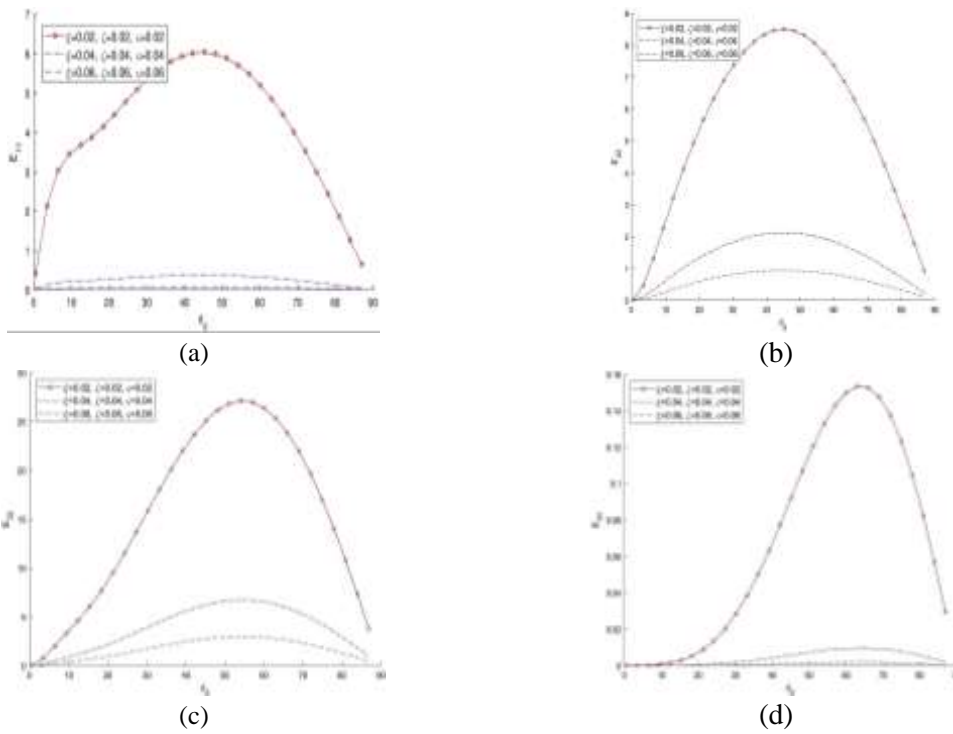


Fig. 4 Effect of nonlocal parameters ξ , ζ , and ψ on energy ratios

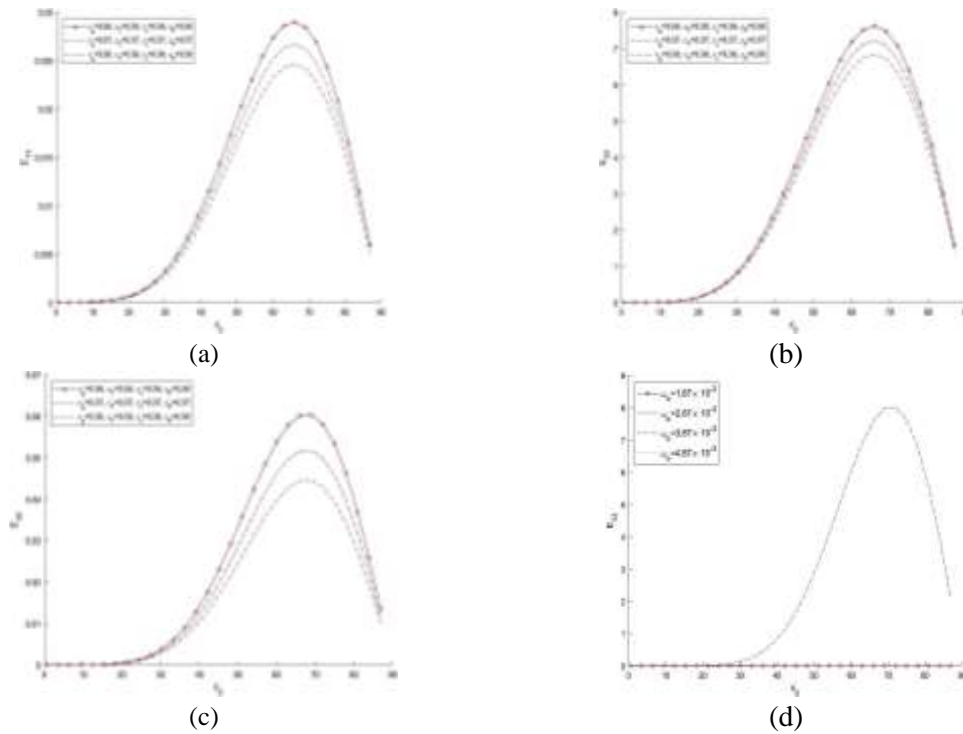


Fig. 5 Effect of phase lag parameters τ_q , τ_T , τ_v and τ_P on energy ratios

perfusion rate. It is found that the sum of energy ratio of the boundary surface is approximately unity at each angle of incidence. This shows that there is no dissipation of energy during the reflection and transmission phenomena at the boundary surface. Phenomena of wave propagation in NL BDS contains significance in field of bio-mechanical engineering for detecting disease.

References

- Achenbach, J.D. (1973), "Wave Propagation in Elastic Solids", North-Holland, Amsterdam.
- Borcherdt, R.D. (1982), "Reflection-refraction of general P and type-I S waves in elastic and inelastic solids", *Geophys. J. Roy. Astron. Soc.*, **70**, 621-638. <https://doi.org/10.1111/j.1365-246X.1982.tb05976.x>.
- Cao, B.Y. and Guo, Z.Y. (2007), "Equation of motion of a phonon gas and non-Fourier heat conduction", *J. Appl. Phys.*, **102**(5), 053503. <https://doi.org/10.1063/1.2775215>.
- Cattaneo, C. (1958), "A form of heat conduction equation which eliminates the paradox of instantaneous propagation", *Comptes Rendus*, **247**, 431-433.
- Chen, P.J., Gurtin M.E. and Williams W.O. (1969), "On the thermodynamics of non-simple elastic materials with two temperatures", *ZAMP*, **20**, 107-112. <https://doi.org/10.1007/BF01591120>.
- Chen, P.J., Gurtin, M.E. and Williams, W.O. (1968), "A note on non-simple heat conduction", *ZAMP*, **19**, 969-970. <https://doi.org/10.1007/BF01602278>.
- Ghanmi, A. and Abbas Ibrahim, A. (2019), "An analytical study on the fractional transient heating within the skin tissue during the thermal therapy", *J. Therm. Biol.*, **82**, 229-233. <https://doi.org/10.1016/j.jtherbio.2019.04.003>.
- Green, A.E. and Lindsay, K.A. (1972), "Thermoelasticity", *J. Elast.*, **2**, 1-7. <https://doi.org/10.1007/BF00045689>.
- Green, A.E. and Naghdi, P.M. (1993), "Thermoelasticity without energy dissipation", *J. Elast.*, **31**(3), 189-208. <https://doi.org/10.1007/BF00044969>.
- Guo, Z.Y. and Cao, B.Y. (2008), "A general heat conduction law based on the concept of motion of thermal mass", *Acta Phys. Sinica*, **7**, 53.
- Guo, Z.Y. and Hou, Q.W. (2010), "Thermal wave based on the thermomass model", *J. Heat Transf.*, **132**(7), 072403. <https://doi.org/10.1115/1.4000987>.
- Guyer, R.A. and Krumhansl, J.A. (1966), "Solution of the linearized phonon boltzmann equation", *Phys. Rev.*, **148**, 766.
- Kim, J.Y., Jang, K., Yang, S.J. and Baek, J.H. (2016), "Simulation study of the thermal and the thermoelastic effects induced by pulsed laser absorption in human skin", *J. Kor. Phys. Soc.*, **68**(8), 979-988. <https://doi.org/10.3938/jkps.68.979>.
- Kumar, D. and Rai, K.N. (2020), "Three-phase-lag bioheat transfer model and its validation with experimental data", *Mech. Base. Des. Struct. Mach.*, 1-15. <https://doi.org/10.1080/15397734.2020.1779741>.
- Kumar, R. and Gupta, V. (2015), "Wave propagation at the boundary surface of inviscid fluid half-space and thermoelastic diffusion solid half-space with dual-phase-lag models", *J. Solid Mech.*, **7**(3), 312-326.
- Kumar, R., Vashishth, A.K. and Ghangas, S. (2019a), "Phase-Lag effects in skin tissue during transient heating", *Int. J. Appl. Mech. Eng.*, **24**(3), 603-623. <https://doi.org/10.2478/ijame-2019-0038>.
- Kumar, R., Vashishth, A.K. and Ghangas, S. (2019b), "Nonlocal heat conduction approach in a bi-layer tissue during magnetic fluid hyperthermia with dual phase lag model", *Bio-Med. Mater. Eng.*, **30**, 387-402. <https://doi.org/10.3233/bme-191061>.
- Lavrentyev, A.I. and Rokhlin, S.I. (1998), "Ultrasonic spectroscopy of imperfect contact interfaces between a layer and two solids", *J. Acoust. Soc. Am.*, **103**, 657. <https://doi.org/10.1121/1.423235>.
- Li, X., Li, C., Xue, Z. and Tian, X. (2018), "Analytical study of transient thermo-mechanical responses of dual-layer skin tissue with variable thermal material properties", *Int. J. Therm. Sci.*, **124**, 459466. <https://doi.org/10.1016/j.ijthermalsci.2017.11.002>.
- Li, X., Li, C., Xue, Z. and Tian, X. (2019), "Investigation of transient thermo-mechanical responses on the

- triple-layered skin tissue with temperature dependent blood perfusion rate”, *Int. J. Therm. Sci.*, **139**, 339-349. <https://doi.org/10.1016/j.ijthermalsci.2019.02.022>.
- Li, X., Xue, Z. and Tian, X. (2018), “A modified fractional order generalized bio-thermoelastic theory with temperature-dependent thermal material properties”, *Int. J. Therm. Sci.*, **132**, 249-256. <https://doi.org/10.1016/j.ijthermalsci.2018.06.007>.
- Li, X., Zhong, Y., Jazar, R. and Subic, A. (2014), “Thermal-mechanical deformation modelling of soft tissues for thermal ablation”, *Biomed. Mater. Eng.*, **24**(6), 2299-310. <https://doi.org/10.3233/BME-141043>.
- Li, X., Zhong, Y., Smith, J. and Gu, C. (2017), “Non-Fourier based thermal-mechanical tissue damage prediction for thermal ablation”, *Bioeng.*, **8**(1), 71-77. <https://doi.org/10.1080/21655979.2016.1227609>.
- Lord, H.W. and Shulman, Y. (1967), “A generalized dynamical theory of thermoelasticity”, *J. Mech. Phys. Solid.*, **15**, 299-309. [https://doi.org/10.1016/0022-5096\(67\)90024-5](https://doi.org/10.1016/0022-5096(67)90024-5).
- Lotfy, K. (2014), “A novel model for photothermal excitation of variable thermal conductivity semiconductor elastic medium subjected to mechanical ramp type with two-temperature theory and magnetic field”, *Sci. Rep.*, **9**, 3319. <https://doi.org/10.1038/s41598-019-39955-z>.
- Lotfy, K. and Hassan, W. (2014), “Normal mode method for two-temperature generalized thermoelasticity under thermal shock problem”, *J. Therm. Stress.*, **37**, 545-560. [https://doi.org/10.1016/0022-5096\(67\)90024-5](https://doi.org/10.1016/0022-5096(67)90024-5).
- Lu, W.Q., Liu, J. and Zeng, Y. (1998), “Simulation of the thermal wave propagation in biological tissues by the dual reciprocity boundary element method”, *Eng. Anal. Boundary Element.*, **22**(3), 167-174. [https://doi.org/10.1016/S0955-7997\(98\)00039-3](https://doi.org/10.1016/S0955-7997(98)00039-3).
- Othman, M.I. and Lotfy, K. (2011), “Effect of rotation on plane waves in generalized thermo-microstretch elastic solid with one relaxation time”, *Multidiscipline Model. Mater. Struct.*, **7**(1), 43-62. <https://doi.org/10.1108/MMMS-11-2012-0026>.
- Othman, M.I.A., Abo-Dahab, S.M. and Lotfy, K. (2014), “Gravitational effect and initial stress on generalized magneto-thermo-microstretch elastic solid for different theories”, *Appl. Math. Comput.*, **230**, 597-615. <https://doi.org/10.1016/j.amc.2013.12.148>.
- Park, C.S., Liu, C., Hall, S.K. and Payne, S.J. (2017), “A thermoelastic deformation model of tissue contracting during thermal ablation”, *Int. J. Hyperthermia*, **34**(3), 221-228. <https://doi.org/10.1080/02656736.2017.1335441>.
- Pennes, H.H. (1948), “Analysis of tissue and arterial blood temperature in the resting forearm”, *J. Appl. Phys.*, **1**, 93-122. <https://doi.org/10.1152/jappl.1948.1.2.93>.
- Roychoudhary S.K. (2007), “On a thermoelastic three-phase-lag model”, *J. Therm. Stress.*, **30**, 231-238. <https://doi.org/10.1080/01495730601130919>.
- Sarkar, N. (2019), “Love waves in a nonlocal elastic media with voids”, *Acta Mech.*, **231**(3), 947-955. <https://doi.org/10.1007/s00707-019-02583-9>.
- Sharma, K. and Marin, M. (2014), “Reflection and transmission of waves from imperfect boundary between two heat conducting micropolar thermoelastic solids”, *Analele Universitatii Ovidius Constanta-Seria Matematica*, **22**(2), 151-176.
- Shen, W., Zhang, J. and Yang, F. (2005), “Modeling and numerical simulation of bioheat transfer and biomechanics in soft tissue”, *Math. Comput. Model.*, **41**(11-12), 1251-1265. <https://doi.org/10.1016/j.mcm.2004.09.006>.
- Sherief, H.H., Hamza, F.A. and Saleh, H.A. (2004), “The theory of generalized thermoelastic diffusion”, *Int. J. Eng. Sci.*, **42**, 591-608. <https://doi.org/10.1016/j.ijengsci.2003.05.001>.
- Shrama, K. (2012), “Reflection of plane waves in thermodiffusive elastic half-space with voids”, *Multidiscipline Model. Math. Struct.*, **8**(3), 269-296. <https://doi.org/10.1108/15736101211269113>.
- Tzou, D.Y. (1995), *Macro-to Microscale Heat Transfer: The Lagging Behavior*, Taylor and Francis, Washington.
- Tzou, D.Y. and Guo, Z.Y. (2010), “Nonlocal behavior in thermal lagging”, *Int. J. Therm. Sci.*, **49**(7), 1133-1137. <https://doi.org/10.1016/j.ijthermalsci.2010.01.022>.
- Vernotte, P. (1958), “Les paradoxes de la theorie continue de l’equation de la chaleur”, *Compt Rendu*, **246**, 3154-3155.

- Wang, Y.Z., Zhang, X.B. and Song, X.N. (2014), "A generalized theory of thermoelasticity based on thermomass and its uniqueness theorem", *Acta Mech.*, **225**(3), 797-808. <https://doi.org/10.1007/s00707-013-1001-4>.
- Xiong, C. and Guo, Y. (2017), "Electromagneto-thermoelastic diffusive plane waves in a half-space with variable material properties under fractional order thermoelastic diffusion", *Int. J. Appl. Electromag. Mech.*, **53**, 251-269. <https://doi.org/10.3233/jae-160038>.
- Xu, F., Lu, T.J. and Seffen, K.A. (2008), "Biothermomechanical behavior of skin tissue", *Acta Mech. Sinica*, **24**(1), 1-23. <https://doi.org/10.1007/s10409-007-0128-8>.
- Xu, F., Seffen, K.A. and Lu, T.J. (2008), "Non-Fourier analysis of skin biothermomechanics", *Int. J. Heat Mass Transf.*, **51**(9-10), 2237-2259. <https://doi.org/10.1016/j.ijheatmasstransfer.2007.10.024>.
- Yu, Y.J., Li, C.L., Xue, Z.N. and Tian, X.G. (2016), "The dilemma of hyperbolic heat conduction and its settlement by incorporating spatially nonlocal effect at nanoscale", *Phys. Lett. A*, **380**, 255-261. <https://doi.org/10.1016/j.physleta.2015.09.030>.
- Yu, Y.J., Tian, X.G. and Xiong, Q.L. (2016), "Nonlocal thermoelasticity based on nonlocal heat conduction and nonlocal elasticity", *Eur. J. Mech. A Solid.*, **60**, 238-253. <https://doi.org/10.1016/j.euromechsol.2016.08.004>.

Appendix

Appendix A

$$\begin{aligned}
 R_1 &= \frac{l_1 T_0 c_0^2}{\omega_1^* k}, & R_2 &= \frac{\gamma_1^2 T_0}{\rho \omega_1^* k}, & R_3 &= \frac{dT_0 b \gamma_1 \gamma_2}{\rho \omega_1^* k}, & R_4 &= \frac{\omega_b \rho_b c_b c_0^2}{\omega_1^{*2} k}, \\
 q_1^* &= \frac{c_0^2}{D b \omega_1^*}, & q_2^* &= \frac{d \rho c_0^4}{\gamma_1 \gamma_2 D b \omega_1^*}, & q_3^* &= \frac{n c_0^2}{D \omega_1^*}, \\
 \tau_{T2} &= (1 - i\omega \tau_T), \tau_{p2} = (1 - i\omega \tau_p), \tau_{q2} = (1 - i\omega \tau_q + (-i\omega)^2 \frac{\tau_q^2}{2}), \\
 \tau_{v2} &= 1 - i\omega \tau_n + (-i\omega)^2 \frac{\tau_n^2}{2}, = R_2 \tau_{q2}, & B &= R_2 \zeta^2, & C &= (R_1 + \frac{R_4}{i\omega}) \tau_{q2}, \\
 D &= -(R_1 + \frac{R_4}{i\omega}) \zeta^2 + \frac{\tau_{T2}}{i\omega}, E = R_3 \tau_{q2}, & F &= R_3 \zeta^2, \\
 G &= \tau_{v2} q_1^*, & H &= \zeta^2 q_1^*, & I &= \tau_{v2} q_2^*, & J &= \zeta^2 q_2^*, & K &= \tau_{v2} q_3^*, \\
 L &= \zeta q_3^* - \frac{\tau_{p2}}{i\omega}.
 \end{aligned}$$

Appendix B

$$\begin{aligned}
 B_1 &= (1 - \omega^2 \xi^2) A_1 - A_7 + \Gamma A_4, & B_2 &= \omega^2 A_1 + (1 - \omega^2 \xi^2) A_2 - A_8 + \Gamma A_5, \\
 B_3 &= A_2 \omega^2 + (1 - \omega^2 \xi^2) A_3 - A_9 + \Gamma A_6, & B_4 &= \omega^2 A_3, \Gamma = \frac{b \gamma_2^2}{\rho c_0^2}, \\
 A_1 &= FJ + DL, & A_2 &= LC - DK - FI - JE, & A_3 &= KI - KC, \\
 A_4 &= BJ + HD, & A_5 &= HC - DG - BI - AJ, & A_6 &= A - CG, \\
 A_7 &= BL - HF, & A_8 &= FG + HE - AL - BK, & A_9 &= AK - EG, \\
 A &= R_2 \tau_{q2}, & B &= R_2 \zeta^2, & C &= (R_1 + \frac{R_4}{i\omega}) \tau_{q2}, \\
 D &= -(R_1 + \frac{R_4}{i\omega}) \zeta^2 + \frac{\tau_{T2}}{i\omega}, & E &= R_3 \tau_{q2}, & F &= R_3 \zeta^2, \\
 G &= \tau_{v2} q_1^*, & H &= \zeta^2 q_1^*, & I &= \tau_{v2} q_2^*, & J &= \zeta^2 q_2^*, & K &= \tau_{v2} q_3^*, \\
 L &= \zeta^2 q_3^* - \frac{\tau_{p2}}{i\omega}, \\
 n_i &= \frac{-(BL - HF)\omega^6 + (FG + HE - AL - BK)\omega^4 V_1^2 - (AK - EG)\omega^2 V_1^4}{(FJ + DL)\omega^4 V_1^2 - (CL - DK - FI - JE)\omega^2 V_1^4 + (EI - KC)V_1^6}, \\
 k_i &= \frac{(BJ + HD)\omega^6 + (HC - DG - BI - AJ)\omega^4 V_1^2 - (A - CG)\omega^2 V_1^4}{(FJ + DL)\omega^4 V_1^2 - (CL - DK - FI - JE)\omega^2 V_1^4 + (EI - KC)V_1^6}, & i &= 1, 2, 3.
 \end{aligned}$$

Appendix C

$$\begin{aligned}
d_{11} &= \frac{i\rho^f c_1^2}{\omega}, d_{1j} = \lambda_0 \left(\frac{\xi_R}{\omega}\right)^2 + \rho c_0^2 \left(\frac{dV_j}{\omega}\right)^2 + \rho c_0^2 \frac{n_j}{\omega^2} + b\gamma_2^2 \frac{k_j}{\omega^2}, d_{15} \\
&= (\rho c_0^2 - \lambda_0) \left(\frac{\xi_R}{\omega}\right) \left(\frac{dV_4}{\omega}\right), \\
d_{21} &= 0, d_{2j} = 2\mu \frac{\xi_R}{\omega} \frac{dV_j}{\omega}, d_{25} = \mu \left[\left(\frac{\xi_R}{\omega}\right)^2 - \left(\frac{dV_4}{\omega}\right)^2 \right], \\
d_{31} &= c_1, \frac{dV_\alpha k_n}{i\omega c_0}, d_{3j} = \lambda_0 \left(\frac{\xi_R}{\omega}\right)^2 + \rho c_0^2 \left(\frac{dV_j}{\omega}\right)^2 + \rho c_0^2 \frac{n_j}{\omega^2} + b\gamma_2^2 \frac{k_j}{\omega^2} - ik_n \frac{dV_j}{\omega}, d_{35} \\
&= (\rho c_0^2 - \lambda_0) \frac{\xi_R}{\omega} \frac{dV_4}{\omega} - ik_n \frac{\xi_R}{\omega}, \\
d_{41} &= 0, \quad d_{4j} = in_j \frac{dV_j}{\omega}, d_{45} = 0, \\
d_{51} &= 0, \quad d_{5j} = ik_j \frac{dV_j}{\omega}, \quad d_{55} = 0, \\
g_1 &= d_{11}, \quad g_i = 0, \quad i = 2,3,4,5, \quad j = 2,3,4.
\end{aligned}$$

Appendix D

$$\begin{aligned}
\langle P_{ij}^* \rangle &= -\frac{\omega^4}{2} \text{Re} \left[2\mu \frac{\xi_R}{\omega} \frac{\xi_R}{\omega} \frac{dV_i}{\omega} + \frac{dV_2}{\omega} \left(\lambda_0 \left(\frac{\xi_R}{\omega}\right)^2 + \rho c_0^2 \frac{dV_1}{\omega} + \frac{\rho c_0^2 n_i}{\omega^2} + \frac{\rho c_0^2 k_i}{\omega^2} \right) Z_i \bar{Z}_j \right], \\
\langle P_{i4}^* \rangle &= -\frac{\omega^4}{2} \text{Re} \left[-2\mu \frac{\xi_R}{\omega} \frac{dV_4}{\omega} \frac{dV_i}{\omega} + \frac{\xi_R}{\omega} \left(\lambda_0 \left(\frac{\xi_R}{\omega}\right)^2 + \rho c_0^2 \left(\frac{dV_i}{\omega}\right)^2 + \frac{\rho c_0^2 n_i}{\omega^2} + \frac{\rho c_0^2 k_i}{\omega^2} \right) Z_i \bar{Z}_4 \right], \\
\langle P_{4j}^* \rangle &= \frac{-\omega^4}{2} \text{Re} \left[\left[\mu \left(\left(\frac{\xi_R}{\omega}\right)^2 - \left(\frac{dV_4}{\omega}\right)^2\right) \frac{\xi_R}{\omega} - \frac{\xi_R}{\omega} \cdot \frac{dV_4}{\omega} + \lambda_0 \frac{dV_j}{\omega} + \frac{\xi_R}{\omega} \frac{dV_4}{\omega} \frac{dV_j}{\omega} \rho c_0^2 \right] Z_4 \bar{Z}_j \right], \\
\langle P_{44}^* \rangle &= \frac{-\omega^4}{2} \text{Re} \left[\left[-\mu \left(\left(\frac{\xi_R}{\omega}\right)^2 - \left(\frac{dV_4}{\omega}\right)^2\right) \frac{dV_4}{\omega} + 2\mu \frac{\xi_R}{\omega} \frac{\xi_R}{\omega} \frac{dV_4}{\omega} \right] Z_4 \bar{Z}_4 \right], \\
& \quad i, j = 1, 2, 3.
\end{aligned}$$